Afshar Vahid, Shahraam; Bao, Xiaoyi; Zou, L.; Chen, L.
Brillouin spectral deconvolution method for centimeter spatial resolution and high-accuracy strain measurement in Brillouin sensors, *Optics Letters*, 2005; 30 (7):705-707.

Brillouin spectral deconvolution method for centimeter spatial resolution and high-accuracy strain measurement in Brillouin sensors

Shahraam Afshar V., Xiaoyi Bao, Lufan Zou, and Liang Chen

Fiber Optics Group, Department of Physics, University of Ottawa, 150 Louis Pasteur, Ottawa, Ontario K1N 6N5, Canada

Received September 22, 2004

Combining a dc and a short pulse (~1 ns) as the probe beam in the pump–probe configuration of Brillouin-based distributed sensors allows us to represent the Brillouin spectrum as a top Lorentzian-like portion and a bottom Gaussian-like portion. Because of the interaction of these two parts, the Lorentzian-like portion carries spatial information that can be extracted within centimeter spatial resolution. Using this information, we develop a spectrum deconvolution method, which considers the location correlation of the strain distribution, to find the number of Brillouin peaks and their frequencies in the top Lorentzian-like portion and hence achieve accurate strain information. An optimum level of dc to pulse power for the best signal and position detection capability is discussed. © 2005 Optical Society of America

OCIS codes: 290.5830, 060.4370, 060.2370.

Pump–probe Brillouin-scattering-based fiber-optic sensors are distributed-strain (temperature) sensors.[1] Strain (temperature) sensing is based on measuring the shift in the central frequency of the Brillouin profile (ν_B), which is linearly proportional to local strain (temperature).[2] The resolution of the shift measurement is determined by a parameter called the minimum detectable Brillouin frequency shift $\delta\nu_B$ (Ref. 3):

$$\delta\nu_B = \frac{\Delta\nu_B}{\sqrt{2}(\mathrm{SNR})^{1/4}}, \tag{1}$$

where $\Delta\nu_B$ is the Brillouin linewidth and SNR is the signal-to-noise ratio. Although this equation is valid for distributed Brillouin sensors with pulses longer than the phonon lifetime and one peak condition, the $\delta\nu_B \propto \Delta\nu_B$ relation is generally valid. Distributed sensing is achieved by Brillouin optical time-domain analysis, in which the spatial resolution is determined by half of the pulse length, $\delta z = cW/2n$, where W is the Stokes pulse width. This indicates that local strain information cannot be resolved within half a pulse length because of the location-correlated strain distribution. The performance of Brillouin sensors can be classified with spatial and strain resolutions, which depend on pulse width, Brillouin profile linewidth, and SNR. Although the spatial resolution can be improved by use of short-pulse probe beams, the resultant Brillouin profile [the convolution of the pulse spectrum and the spontaneous Brillouin gain spectrum $g_B(\nu)$] is broadened to a Gaussian-like profile as the pulse width decreases below the phonon lifetime,[3] thus reducing the accuracy of strain measurements through Eq. (1). On the other hand, high-accuracy strain measurement is achievable using long pulses, because of their resultant narrow Lorentzian-like spectra and hence smaller $\delta\nu_B$ in Eq. (1), at the cost of degrading the spatial resolution since the obtained strain values represent only the spatially correlated strain distribution over the half-pulse length. Hence it was generally believed that simultaneous submeter resolutions and high-accuracy strain measurements were unachievable because the rapid linewidth increases when $W < \tau_{\mathrm{phonon}} = 10$ ns (half-pulse length 1 m).

In this Letter, using a numerical model of stimulated Brillouin scattering in optical fiber,[4,5] we propose a new Brillouin spectral deconvolution method for a combination of a dc and a short pulse as the probe beam in the pump–probe configuration of Brillouin sensors to achieve both high-accuracy strain measurements and centimeter spatial resolution. Using this approach, we extract spatial information with a resolution better than the half-pulse length (in the centimeter range). This information is then employed to deconvolute the strain distribution to less than the half-pulse length, which otherwise is correlated over the whole fiber length. For this study we use a probe beam consisting of a 1-ns pulse (half-pulse length of 10 cm) and a dc portion with another cw beam as the pump. We quantify the ratio of the dc and pulse powers in the probe laser beam with extinction ratio R_x defined as $R_x = (p_{\mathrm{pulse}} + p_{\mathrm{dc}})/p_{\mathrm{dc}}$. Experimentally, one can control the extinction ratio by adjusting the bias voltage of an electro-optic modula-

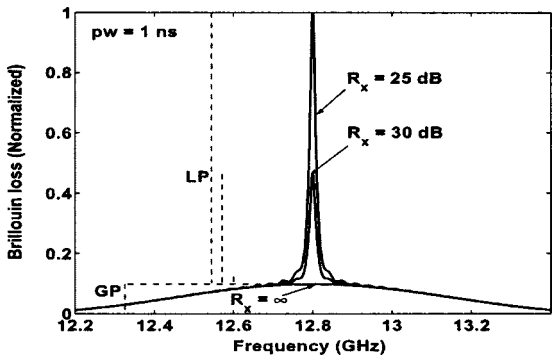

Fig. 1. Typical twofold Brillouin profiles of a point inside a 600-cm fiber for different extinction ratios. Finite R_x curves consist of both Gaussian-like and Lorentzian-like portions labeled as GP and LP.

0146-9592/05/070705-3/$15.00

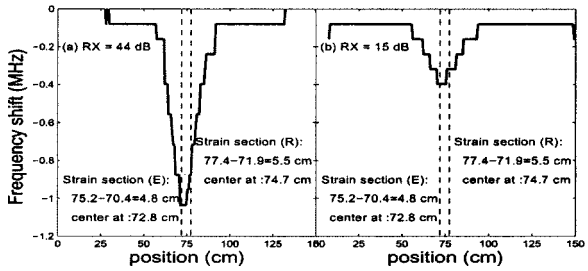

Fig. 2. Brillouin profile shift as a function of position inside a 150-cm fiber with a 5.5-cm strained section. Real (R and dashed lines) and estimated (E) strain sections are shown.

tor. The resultant Brillouin spectrum of such a combined probe–pump interaction consists of two portions[4]: a top Lorentzian-like portion, representing the dc–pump interaction and a bottom Gaussian-like portion representing the pulse–pump interaction, as is evidenced in Fig. 1. In Fig. 1 the $R_x=\infty$ curve shows a broad Gaussian-like profile owing to a short ($W=1$ ns $<\tau$) pulse–pump interaction. The other profiles, typical of all finite extinction ratio cases however, show twofold spectral profiles consisting of the bottom Gaussian-like profile of $R_x=\infty$ plus a top narrower Lorentzian-like profile. The strength of the pulse–pump and dc–pump interactions and hence the ratio of the Lorentzian- and Gaussian-like powers, LP and GP in Fig. 1, as well as the Gaussian-like linewidth can be controlled by R_x and the pulse width, respectively. The Gaussian-like part of the profile provides localized strain information, spatially correlated over the half-pulse length, whereas the Lorentzian-like portion contains accurate (because of its narrow linewidth) but nonlocalized (spatially correlated over the whole fiber length) strain information. For a finite extinction ratio the Lorentzian-like part of the profile has two contributions: one owing to cw–cw interaction outside the pulse length, and the other owing to cw–cw interaction within the pulse length combined with the pulse–cw interaction. The first interaction provides nonlocalized information and hence is position independent, whereas the second interaction provides localized information and is position dependent. Therefore the overall Lorentzian-like part of the Brillouin profile also varies as a function of position because of its position-dependent contribution.

With the above key concept of combined dc and pulse probe–pump interaction, our new method consists of two stages: (1) By examining the variation in the Lorentzian-like portion as a function of position and finding the position of maximum change, we extract the spatial information for the existing strain sections of the fiber and a rough estimate of their strain values, and (2) the information obtained in stage (1) is used to deconvolute the top Lorentzian-like portion into its primary Lorentzian peaks and thus extract accurate strain information for the existing strain sections. In this way stage (1) provides centimeter spatial resolution, whereas stage (2) provides accurate strain information. Using this method, we detect the position and frequency shift of a short strained section of 5.5 cm, shifted by −3.2 MHz, in the middle of a 150-cm, strain-free (0-MHz shift) optical fiber. Similar to Fig. 1, the Brillouin profile has a twofold structure consisting of a bottom Gaussian-like portion and a top Lorentzian-like portion. Since the top Lorentzian-like portion represents the cw–cw interaction all over the fiber, for this example, it is the combination of two individual Lorentzians, one representing the cw–cw interaction in the strain region (5.5 cm) and the other representing the cw–cw interaction in the rest of the fiber (144.5 cm). Generally, combination of two different Lorentzian functions $A^2/[1+(\nu-\nu_{B1})^2/\Delta\nu_1^2]$ and $B^2/[1+(\nu-\nu_{B2})^2/\Delta\nu_2^2]$ can generate a profile with either two distinctive shifted peaks or one shifted peak (Lorentzian-like) between ν_{B1} and ν_{B2}. The frequency shift in both cases depends on $\nu_{B2}-\nu_{B1}$, the linewidths, and the heights of the original Lorentzian functions. In this example, since the Brillouin frequency difference of the strained and nonstrained sections (−3.2 MHz) is small, the Lorentzian-like portion of the twofold Brillouin profile of any point along the fiber shows only one shifted peak that includes the strain information of the point (resulting from pulse–cw and cw–cw interactions within the pulse length) and the strain information for the rest of the fiber. Therefore the maximum contribution of the strained section to the twofold profile occurs at points close to or inside the strained section since those profiles have the highest contribution of pulse–cw interaction of the strained section. As the first stage of our method, we have examined the frequency shift of the overall Lorentzian-like portion of the Brillouin profile as a function of position for two different values of extinction ratios as shown in Fig. 2. Figure 2(a) resembles a maximum Brillouin shift of −1.0 MHz over the range 71.1−74.5 cm, which can be considered the strained section, overlapping the real strained section that extends from 71.9 to 77.4 cm. This clearly indicates that the first stage of our method is successful in detecting the position of the strained section. This stage, however, does not provide accurate strain information for the section (compare the detected shift of −1.0 MHz with the real shift of −3.2 MHz). The first stage also provides valuable information such as the number of existing strained sections and their frequency ranges for the second stage. For example, Fig. 2 indicates that the fiber consists of two sections, one with a small frequency shift of the order of

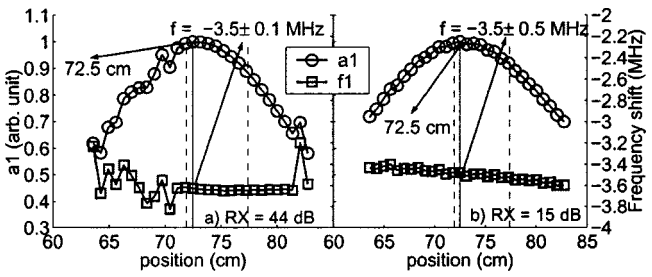

Fig. 3. a_1 and f_1 as a function of position. Dashed lines show the real strained section extending between 71.9 and 77.4 cm, and the solid curve indicates the estimated strain center and its frequency shift.

Table 1. Results for Detection of a 5.5-cm Strained Section (Extending from 71.9 to 77.4) with a Frequency Shift of −3.2 MHz

Parameter	Stage	Values			
Rx (dB)		44	34	24	15
Detected section	(1)	74.5–71.1	73.8–71.8	74.5–71.8	77.4–71.9
Detected *f* (MHz)	(1)	−1.0	−0.9	−0.6	−0.4
Detected *f* (MHz)	(2)	−3.5±0.1	−3.5±0.2	−3.7±0.3	−3.5±0.5
Relative error	(2)	3%	6%	8%	14%
LP/GP		10.4 dB	15.6 dB	21.9 dB	29.4 dB

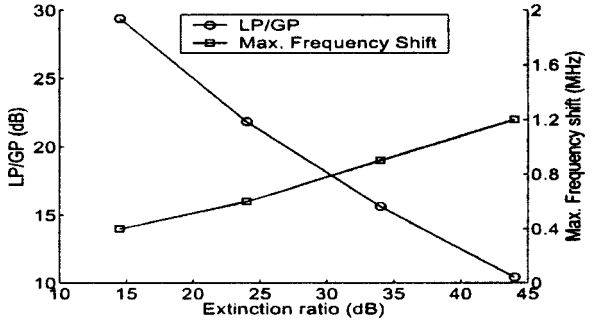

Fig. 4. LP/GP and maximum frequency shifts for the example in Fig. 2 are shown as a function of R_x.

0 MHz and the other with a frequency shift of <-1.0 MHz. This information, together with the height of the top Lorentzian-like portion as a function of position, can be employed in stage (2) to fit a two-Lorentzian function of the form $h(z,f)=a_1/[1+(f-f_1)^2/\Delta f_1^2]+a_2/[1+(f-f_2)^2/\Delta f_2^2]+a_0$ with the constrained parameters a_1, a_2, f_1, f_2, Δf_1, Δf_2, and a_0, in which a_1 and a_2 are the amplitudes, f_1 and f_2 are the central frequencies, Δf_1 and Δf_2 are the linewidths, and a_0 is the offset term to the top Lorentzian-like portion of the profile. The key point of the above discussion is that a_1 and a_2 are functions of z, and more specifically they have a maximum whenever z is in a section in which its frequency shifts match f_1 and f_2, respectively. Figures 3(a) and 3(b) show the results of fitting parameters a_1 and f_1 as a function of z for extinction ratios of 44 and 15 dB. In each case position z and the frequency corresponding to the maximum of a_1 were identified as the center and the frequency shift of the strained section, respectively. The estimated frequency shift of the strained section [see Fig. 3(a)], i.e., $f=-3.5\pm0.1$ MHz is off by only 0.3 MHz compared with the real frequency shift of $f=-3.2$ MHz, which indicates a much better frequency estimation than the first stage. Overall, the results of both stages (1) and (2), summarized in Table 1, demonstrate the capability of our method to detect the position and frequency shift of the example strained section. In real experiments noise can be digitally filtered to smooth the Brillouin profile before using our method. Our method will still be valid since the parameters of the fitting function in the second stage can be constrained to a small range using the information from the first stage.

The extinction ratio is a key parameter that determines the capability of our method in detecting the position and the frequency of a strained section. A higher extinction ratio [Fig. 2(a)] induces a higher maximum frequency shift of the Lorentzian-like portion and hence better position detectability. Although true, this has a drawback since the level of the Lorentzian-like portion relative to the Gaussian-like portion drops for high extinction ratios, as evidenced in Fig. 1. As a result, increasing the extinction ratio reduces the SNR of the Lorentzian-like portion and hence increases the minimum detectable frequency shift $\delta\nu_B$ in Eq. (1). The increase of the extinction ratio eventually turns the Brillouin profile into a broad Gaussian-like profile that degrades the frequency shift measurement because of the large $\Delta\nu_B$ in Eq. (1). This can be demonstrated by plotting the LP/GP ratio $[10\times\log(\mathrm{LP/GP})]$ and the maximum frequency shifts detected in stage (1) (Table 1) as a function of the extinction ratio, shown in Fig. 4. This graph, which can be obtained for any experimental geometry, shows the reduction of the Lorentzian-like signal level to the Gaussian-like level but an increase in the maximum frequency shift as a function of the extinction ratio, and hence it can be used to determine the parameter regime for optimum LP/GP and position detection. In a real experiment, noise associated with thermal, shot, and different devices should also be considered to determine a proper extinction ratio level.

In summary, by combining a dc and a short pulse (1 ns) as the probe beam in a pump–probe Brillouin sensor system, strain sections smaller than the half-pulse length are detectable with a frequency error of ~0.3 MHz within 150 cm of fiber.

The authors thank the National Capital Institute of Telecommunications, the Natural Sciences and Engineering Research Council, and Intelligent Sensing for Intelligent Structures Canada for their support.
S. Afshar V.'s e-mail address is safshar@uottawa.ca

References

1. X. Bao, A. Brown, M. DeMerchant, and J. Smith, Opt. Lett. **24**, 510 (1999).
2. T. Kurashima, T. Horiguchi, and M. Tateda, Appl. Opt. **29**, 2219 (1990).
3. T. Horiguchi, K. Shimizu, T. Kurashima, M. Tateda, and Y. Koyamada, J. Lightwave Technol. **13**, 1296 (1995).
4. S. Afshar V., G. A. Ferrier, X. Bao, and L. Chen, Opt. Lett. **28**, 1418 (2003).
5. V. Lecoeuche, D. J. Webb, C. N. Pannell, and D. A. Jackson, Opt. Lett. **25**, 156 (2000).